Journal of Biomedical Science (2007) 14:129–143
DOI 10.1007/s11373-006-9122-6

Tachyphylaxis to the inhibitory effect of L-type channel blockers on ACh-induced $[Ca^{2+}]_i$ oscillations in porcine tracheal myocytes

Wen-Shuo Chung & Jerry M. Farley*
Department of Pharmacology and Toxicology, University of Mississippi Medical Center, 2500 N. State St., Jackson, MS, 39216-4505, USA

Received 19 August 2006; accepted 19 September 2006

Key words: calcium oscillations, L-type, NCX, smooth muscle, trachea

Summary

Discrepancies about the role of L-type voltage-gated calcium channels (VGCC) in acetylcholine (ACh)-induced $[Ca^{2+}]_i$ oscillations in tracheal smooth muscle cells (TSMCs) have been seen in recent reports. We demonstrate here that ACh-induced $[Ca^{2+}]_i$ oscillations in TMCS were reversibly inhibited by three VGCC blockers, nicardipine, nifedipine and verapamil. Prolonged (several minutes) application of VGCC blockers, led to tachyphylaxis; that is, $[Ca^{2+}]_i$ oscillations resumed, but at a lower frequency. Brief (15–30 s) removal of VGCC blockers re-sensitized $[Ca^{2+}]_i$ oscillations to inhibition by the agents. Calcium oscillations tolerant to VGCC blockers were abolished by KB-R7943, an inhibitor of the reverse mode of Na^+/Ca^{2+} exchanger (NCX). KB-R7943 alone also abolished ACh-induced $[Ca^{2+}]_i$ oscillations. Enhancement of the reverse mode of NCX via removing extracellular Na^+ reversed inhibition of ACh-induced $[Ca^{2+}]_i$ oscillations by VGCC blockers. Inhibition of non-selective cation channels using Gd^{3+} slightly reduced the frequency of ACh-induced $[Ca^{2+}]_i$ oscillations, but did not prevent the occurrence of tachyphylaxis. Altogether, these results suggest that VGCC and the reverse mode of NCX are two primary Ca^{2+} entry pathways for maintaining ACh-induced $[Ca^{2+}]_i$ oscillations in TSMCs. The two pathways complement each other, and may account for tachyphylaxis of ACh-induced $[Ca^{2+}]_i$ oscillations to VGCC blockers.

Introduction

Agonist-induced oscillations in free intracellular calcium concentration ($[Ca^{2+}]_i$) have been observed in a wide range of cell types, and have been linked to a variety of different cellular functions [1–6]. In tracheal smooth muscle cells (TSMC), the frequency and amplitude of $[Ca^{2+}]_i$ oscillations induced by acetylcholine (ACh) was shown to correspond with the development of contractile force in the muscle strip [1, 7]. During agonist-induced $[Ca^{2+}]_i$ oscillations, Ca^{2+} content in the SR/ER is generally not depleted [8]. Nonetheless, Ca^{2+} entry from the extracellular space seems to be indispensable for the maintenance of $[Ca^{2+}]_i$ oscillations [8, 9]. Voltage-gated L-type Ca^{2+} channels (VGCC) are one of the most studied, and well-defined Ca^{2+} entry pathways. However, since $[Ca^{2+}]_i$ oscillations are also observed in non-excitable cells, this voltage-gated channel is not generally considered a major route of Ca^{2+} entry during $[Ca^{2+}]_i$ oscillations. Even in smooth muscle cells, the role of L-type Ca^{2+} entry in $[Ca^{2+}]_i$ oscillations has been controversial, especially in airway smooth muscle. L-type channel blockers are relatively ineffective in treating bronchoconstriction [10]. In tracheal smooth muscle strips, only tension induced by ACh at concentrations

*To whom correspondence should be addressed. Fax: +1-601-984-1637; E-mail: jfarley@pharmacology.umsmed.edu

less than 1 μM were effectively inhibited by L-type channel blockers [11, 12]; with higher concentrations of ACh the inhibition of tension by L-type channel blockers was either partial or insignificant.

Discrepancies about the role of L-type VGCC in agonist-induced $[Ca^{2+}]_i$ oscillations may be attributed to differences in tissue or cell types. However, recent reports about ACh-induced $[Ca^{2+}]_i$ oscillations in TSMC seemed to create a plain discrepancy in the effect of L-type channel blockade in the same type of cell. Sieck and coworkers found that in TSMCs $[Ca^{2+}]_i$ oscillations induced by 1 μM ACh were completely abolished by 100 nM nifedipine, an L-type channel blocker [13]. Using the same tissue, Dai et al. [14] demonstrated that 10 μM nifedipine only partially inhibited the ongoing $[Ca^{2+}]_i$ oscillations, whereas the nifedipine-insensitive component of ACh-induced $[Ca^{2+}]_i$ oscillations was completely abolished by the inhibitors of store-operated non-selective cation channel (NSCC) and Na^+/Ca^{2+} exchanger (NCX). In the latter report, the authors ascribed this discrepancy to the difference in sample preparation. The former used isolated single cells, while the latter measured calcium in cells in intact muscle strips. It is feasible that, as explained in the latter report, the difference in findings might be due to the disruption of intercellular communication, or changes in surface proteins as a result of enzymatic digestion. Our recent observations, however, suggest that the disparity may also stem from tachyphylaxis, or quick adaptation of ACh-induced $[Ca^{2+}]_i$ oscillations to L-type channel blockers.

In the present study, we demonstrate the temporary abolition of ACh-induced $[Ca^{2+}]_i$ oscillations by three different L-type channel blockers (nicardipine, nifedipine, and verapamil), and the development of tachyphylaxis to these three agents. We also examine the roles of NCX and NSCC in tachyphylaxis of ACh-induced $[Ca^{2+}]_i$ oscillations to L-type channel blockers.

Methods

Cell preparation

Porcine tracheae were obtained from a local abattoir. The trachea was dissected free of epithelium, glands and connective tissue. The smooth muscle was then removed from the cartilage and put in physiological saline solution (PSS). The tissue was kept at 4 °C, and digested within 48 h.

For cell dissociation, a smooth muscle strip of about 1–2 rings was first incubated at 37 °C in 10 ml of PSS containing 1.2 mg/ml collagenase type 4 (Worthington) held in a 50 ml tube for 30 min. During incubation, the 50 ml tube that held the enzyme solution was fixed on an angled holder, and rotated at 14–16 rpm. The partially digested tissue was subsequently transferred to another enzyme solution with 10 ml PSS containing 1 mg/ml protease (Sigma) and incubated for 15 min. Finally, the partially digested tissue was transferred to the last enzyme solution with 10 ml PSS containing 1.2 mg/ml collagenase type 4 (Worthington). After incubation at 37 °C for another 30 min, digestion was stopped by mixing the enzyme solution with 20 ml of 4 °C PSS. Single cells were, then, dispersed by trituration. The dissociated cells were filtered with 100 μm cell strainer (Falcon). The filtered solution was diluted with PSS, centrifuged and re-suspended in PSS to remove enzyme. The isolated smooth muscle cells were kept at 4 °C, and used within 24 h.

For Ca^{2+} imaging, cells were plated on a clean glass coverslip (22×22 mm^2, No. 0) held in a chamber fabricated in our departmental machine shop. The coverslips used were cleaned in 1 N HCl overnight to improve the attachment of cells to the glass. Cells were allowed to sediment and attach to the coverslip for 20–30 min at room temperature before being incubated with Ca^{2+}-sensitive fluorescence dye Fluo 4 AM.

Cytosolic Ca^{2+} measurement

Cells were loaded with the Fluo 4 by incubation with the cell-permeant AM ester of Fluo 4 (3 μM in PSS; 3 mM stock solution was prepared in DMSO) at 37 °C for 15 min before being washed with PSS. Cells were illuminated at 488 nm. Fluo 4 fluorescence was measured at ~510 nM. An inverted microscope (Nikon) with 60× (NA: 1.4), or 100× (NA: 1.3) oil-immersion objective lens was used to visualize the cells. Fluorescence was captured by an intensifier (MTI GENIISYS) coupled with a CCD camera (MTI CCD72). The shutter and gain of the intensifier were respectively set at 1 and 200. Images were transmitted to a personal computer and acquired at 5–10 frames per second through a Data Translation DT3155

board. Data were analyzed using Imaging Workbench 5.0 (INDEC Systems, Inc). The fluorescence intensity in a region of interest was defined as the average of the pixel values over the region of an image. The intensity of Ca^{2+} signal was expressed as F/F_0, where F is the fluorescence intensity recorded during the course of experiment, and F_0 is the average fluorescence intensity over 30 s before application of any stimulants.

Perfusion system

The whole cell chamber was continuously perfused with PSS at 2–3 ml/min throughout the experiments. Additional treatments were delivered through a quartz capillary using a DAD-12 superfusion system (ALA Scientific Instruments) to the targeted cells. The tip of the quartz capillary was positioned near the edge of the field under microscope with the targeted cells positioned at the center of the field. The valves and driving pressure of DAD-12 superfusion system were controlled by a laptop running the program DADPORT.

Solutions and chemicals

Normal physiological saline solution (PSS) used in this study contained (mM): 145 Na^+, 5 K^+, 154 Cl^-, 2 Ca^{2+}, 5.5 glucose, 10 HEPES (pH = 7.4). For zero Ca^{2+} buffer, 2 mM Ca^{2+} was substituted with equimolar of Mg^{2+}, and 0.5 mM EGTA was added. For zero Na^+ buffer, Na^+ was replaced with equimolar of *N*-methyl-D-glucamine ($NMDG^+$). All chemicals were purchased from Sigma Chemical Co., except verapamil (Research Biochemical Inc.), KB-R7943 (Calbiochem), and fluo 4 AM (Molecular Probes). Stock solutions (1000×) of all three L-type channel blockers and KB-R7943 were prepared in dimethyl sulfoxide (DMSO).

Data analysis

Data for the effect of each treatment versus control were analyzed using paired *t*-test. Data normalized to controls were analyzed using one-way ANOVA, with Bonferroni corrections when repeated comparisons were made. Data are presented as Mean ± SE, and n = number of cells tested.

Results

ACh-induced $[Ca^{2+}]_i$ oscillations demonstrate tachyphylaxis to the effect of L-type Channel Blockade

Short-term application of L-type channel blockers to ongoing $[Ca^{2+}]_i$ oscillations induced by 1 μM ACh resulted in immediate abolition of $[Ca^{2+}]_i$ oscillations (Figure 1A). In the continuous presence of ACh, $[Ca^{2+}]_i$ oscillations resumed after the removal of L-type channel blockers (Figure 1A). In our experiments, targeted single cells were perfused with the DAD12 Superfusion System. When the tip of the quartz capillary of this microperfusion system was positioned close to the target cells (within 100 micron), agents with desired concentrations could reach the targeted cells in less than 0.1 s. This allowed us to see the inhibitory effect of L-type channel blockers within 1 or 2 s after the target cells were exposed to these agents. In our experience, the same short-term inhibition of $[Ca^{2+}]_i$ oscillations can be repeatedly seen as long as the oscillations last. Even in cells that responded to ACh with non-oscillatory increases in $[Ca^{2+}]_i$, L-type channel blockers were able to reduce the $[Ca^{2+}]_i$ level to near baseline as exemplified by nicardipine (Figure 1B). All these results suggest that Ca^{2+} influx through L-type VGCC is required for the maintenance of $[Ca^{2+}]_i$ oscillations. Further study using 10 μM ACh, however, demonstrated that, while L-type channel blockers (10 μM nicardipine) abolished $[Ca^{2+}]_i$ oscillations induced by 1 μM ACh, they failed to block the transients induced by 10 μM ACh (Figure 2A). This result indicates that L-type Ca^{2+} entry was important only for $[Ca^{2+}]_i$ oscillations induced by lower concentration (≤ 1 μM) of ACh, which is in agreement with the previous reports about the effect of L-type channel blockers on ACh-induced increased intracellular Ca^{2+} and contraction [11, 12]. Even in the absence of external Ca^{2+}, 10 μM ACh was able to evoke $[Ca^{2+}]_i$ transients, though they soon ceased (Figure 2A). We further compared the effects of L-type channel blockade and Ca^{2+} deprivation on $[Ca^{2+}]_i$ transients induced by 10 μM ACh (Figure 2B). The integral of cytosolic Ca^{2+} change (area under curve, but above baseline) over the first minute after initiation of 10 μM ACh was normalized to that over the last minute of 1 μM

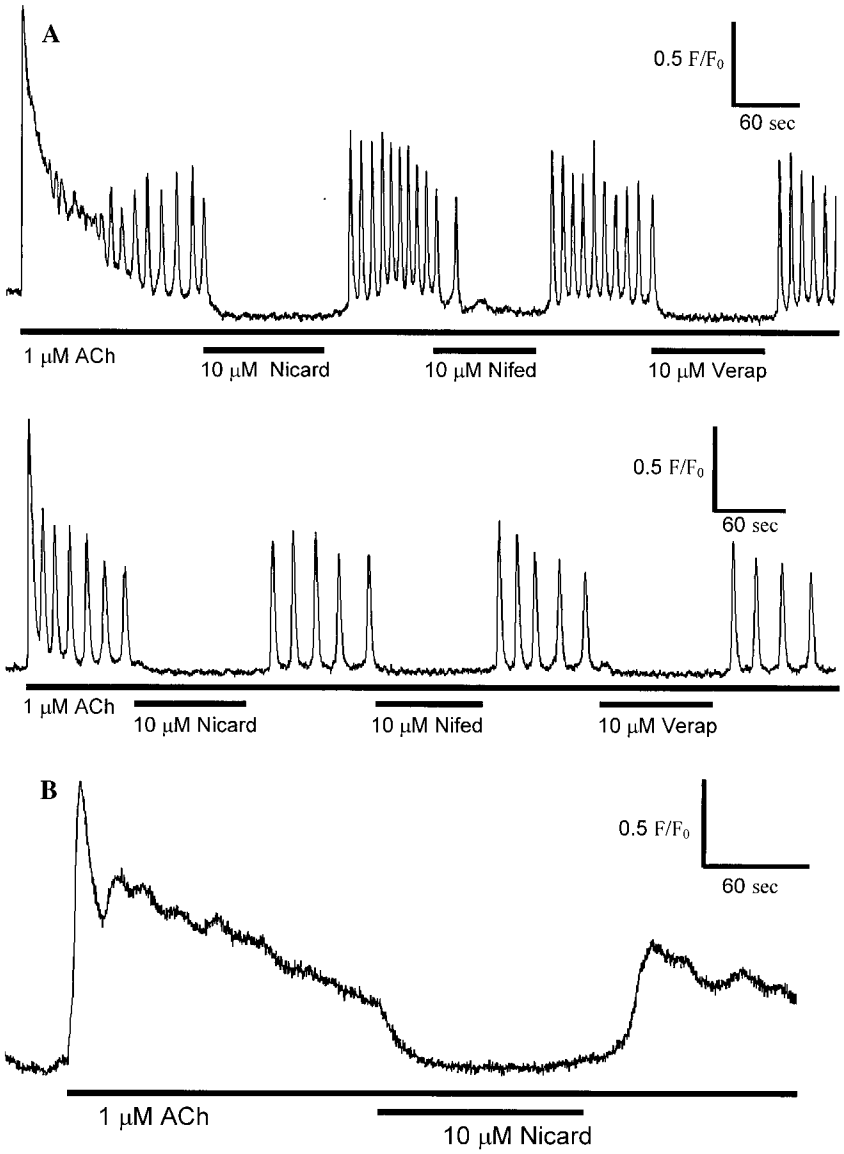

Figure 1. Short-term effect of L-type channel blockers on ACh-induced $[Ca^{2+}]_i$ oscillations, and increase in $[Ca^{2+}]_i$. (A): Two examples are shown, one from a cell that was exposed to ACh for the first time (upper), the other from a cell that had been pre-exposed to ACh, and washed in PSS before the trace as shown was recorded (lower). Both demonstrate that $[Ca^{2+}]_i$ oscillations induced by 1 μM ACh were rapidly and reversibly inhibited by three different L-type channel blockers: nicardipine (Nicard 10 μM), nifedipine (Nifed 10 μM), and verapmil (Verap 10 μM). The $[Ca^{2+}]_i$ traces shown are representative of results in 9 cells from three different animals. Similar results with only one or two of the three channel blockers being applied to each cell were observed in >50 cells from nine animals. (B): In cells where ACh induced a non-oscillatory increase in $[Ca^{2+}]_i$, nicardipine also abolished the steady-state increase in $[Ca^{2+}]_i$ (representative of results in 7 cells from three different animals).

ACh alone treatment (Figure 2A). After normalization, the value for the effect of 10 μM nicardipine is 125.3 ± 8.0%, which is significantly larger than that (70.6 ± 7.2%) for the effect of Ca^{2+} deprivation (***$p < 0.001$, $n = 5$ cells from two animals, Figure 2B). This indicates that in addition to L-type VGCC, there were still other pathways of Ca^{2+} entry which were involved in ACh-induced $[Ca^{2+}]_i$ oscillations.

While short-term application of L-type channel blockers was effective in inhibiting $[Ca^{2+}]_i$ oscillations induced by 1 μM ACh, tachyphylaxis was seen after more prolonged application. As can be seen in Figure 3, ACh-induced $[Ca^{2+}]_i$ oscillations

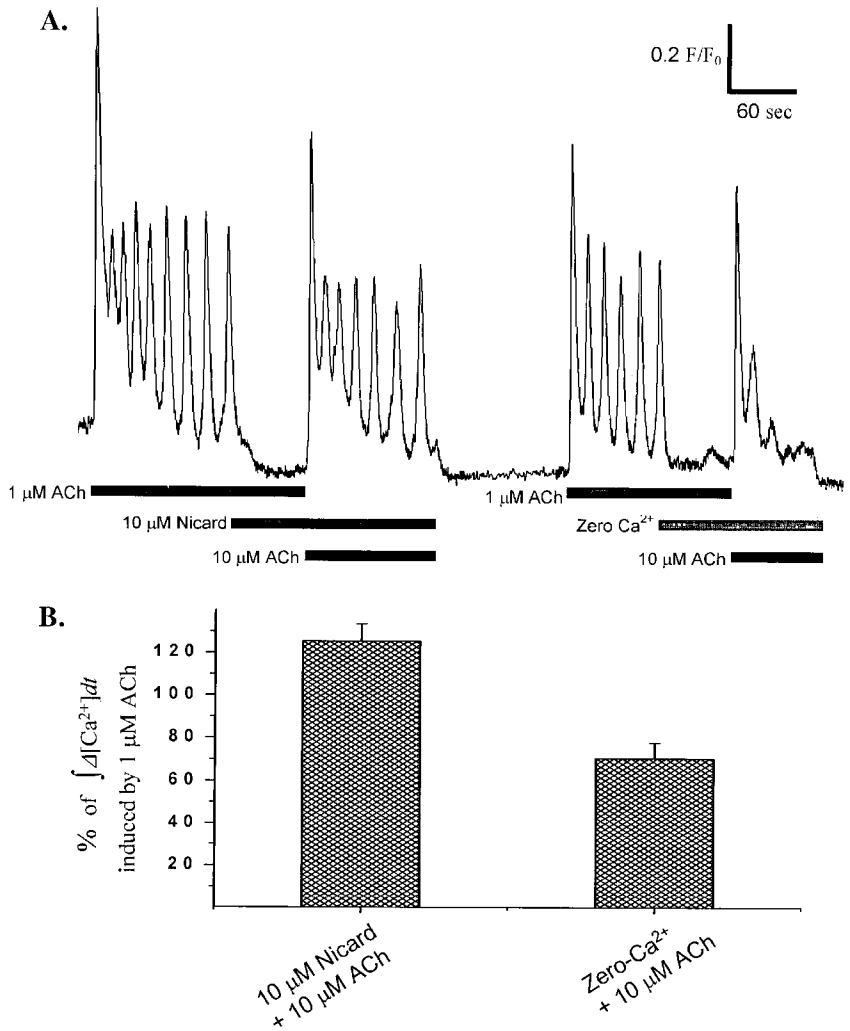

Figure 2. Effects of L-type channel blockade and deprivation of external Ca^{2+} on $[Ca^{2+}]_i$ transients induced by ACh. (A): While nicardipine (10 μM) and Ca^{2+} deprivation abolished $[Ca^{2+}]_i$ oscillations induced by 1 μM ACh, they failed to block Ca^{2+} transients induced by 10 μM ACh. This demonstrates that the abolition of $[Ca^{2+}]_i$ oscillations induced by 1 μM ACh did not result from depletion of the internal Ca^{2+} stores. Comparison between the results of L-type channel blockade and Ca^{2+} deprivation also suggests the existence of another Ca^{2+} entry pathway other than L-type VGCC during $[Ca^{2+}]_i$ oscillations. The $[Ca^{2+}]_i$ trace shown is representative of results in 5 cells from two different animals. (B): The integral of Ca^{2+} change (area under curve, but above baseline) over the first minute after initiation of 10 μM ACh was normalized to that over the last minute of 1 μM ACh alone treatment (A). After normalization, the value for the effect of 10 μM nicardipine is 125.3 ± 8.0%, which is significantly larger than that (70.6 ± 7.2%) for the effect of Ca^{2+} deprivation (***$p < 0.001$, $n = 5$ cells from two animals).

demonstrated tachyphylaxis to the inhibition by verapamil, nifedipine and nicardipine (1–10 μM). Although ACh-induced $[Ca^{2+}]_i$ oscillations were initially abolished by all three L-type channel blockers, oscillations resumed with a lower frequency within a few minutes in the continuous presence of each L-type channel blocker (Figure 3A). Furthermore, after temporary exposure and tolerance developed to a higher concentration (10 μM) of L-type channel blockers, the lower concentration (1 μM) of those agents became ineffective (Figure 3A) in inhibiting $[Ca^{2+}]_i$ oscillations, which is typical of the development of drug tolerance. The time required for the ACh-induced $[Ca^{2+}]_i$ oscillations to resume in the presence of 1 μM of each L-type channel blocker was compared in Figure 3B. The data showed that 1 μM nicardipine is most effective among them in inhibiting $[Ca^{2+}]_i$ oscillations. It took significantly longer for $[Ca^{2+}]_i$ oscillations to resume in the

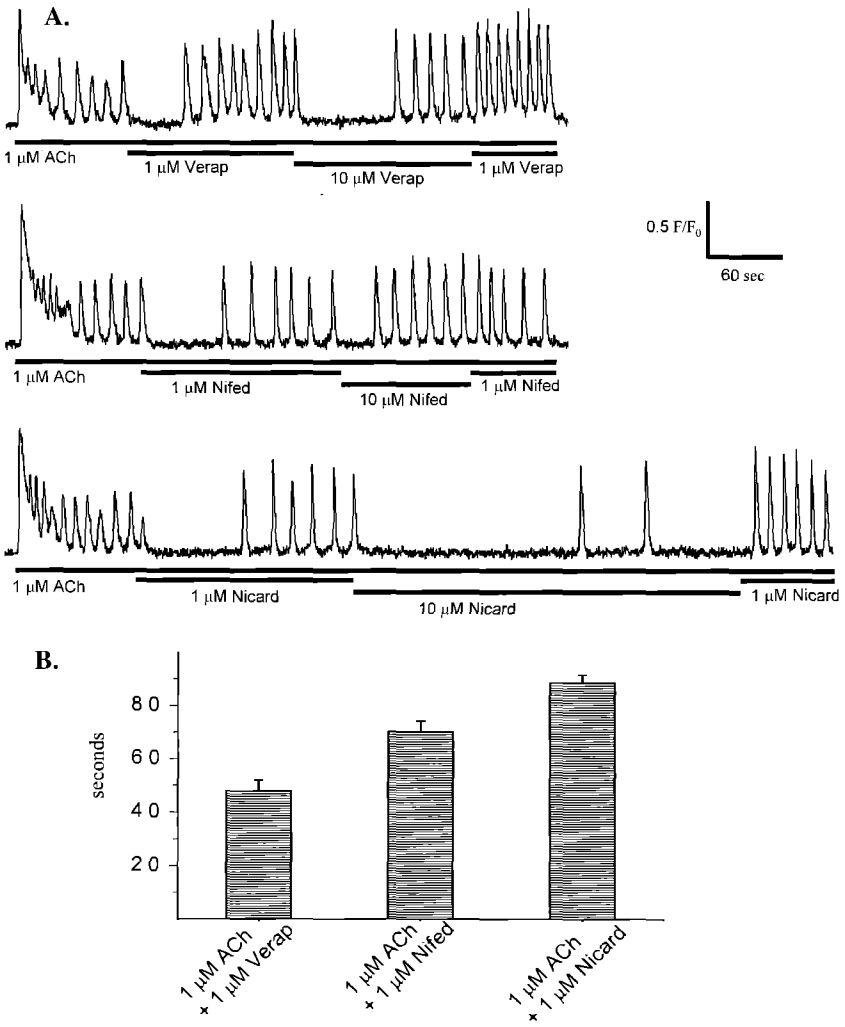

Figure 3. Tachyphylaxis, or quick adaptation of ACh-induced $[Ca^{2+}]_i$ oscillations to the inhibitory effect of L-type channel blockers. (A): ACh-induced $[Ca^{2+}]_i$ oscillations were initially blocked by all three L-type channel blockers each at 1 μM. Yet, within 1–2 min, Ca^{2+} transients reappeared, and oscillations resumed at a lower frequency. The $[Ca^{2+}]_i$ oscillations after resumption were blocked again when the concentration of L-type channel blockers was increased to 10 μM. However, after some time, Ca^{2+} transients reappeared. The three $[Ca^{2+}]_i$ traces shown are three sections from one recording on the same cell separated by 3 min of wash in PSS. The $[Ca^{2+}]_i$ traces shown are representative of results in 60 cells from two animals. Similar results with only one or two of the three channel blockers being applied to each cell were observed in >30 cells from six animals. (B): The time required before the recovery of $[Ca^{2+}]_i$ oscillations in the presence of 1 μM of each L-type channel blocker was compared. Calcium transients reappeared significantly faster with verapamil than with nifedipine and nicardipine (**$p < 0.01$, verapamil vs. nifedipine; ***$p < 0.001$, verapamil vs. nicardipine; $n = 6$).

presence of 1 μM nicardipine (89 ± 3 s; ***$p < 0.001$), and 1 μM nifedipine (70 ± 4 s; **$p < 0.01$) as compared to 1 μM verapamil (48 ± 4 s) ($n = 6$ cells from two animals; Figure 3B), which conformed to the order of IC_{50} of these three L-type channel blockers (verapamil > nifedipine > nicardipine) reported previously [15]. The frequency of $[Ca^{2+}]_i$ oscillations recovered from the inhibitions of 1 μM verapamil, nifedipine, and nicardipine were, respectively, 91 ± 15%, 64 ± 5%, and 63 ± 4% of that of their respective control (ACh alone, before inhibition). Using paired t-test, the frequencies of $[Ca^{2+}]_i$ oscillations recovered from 1 μM of nifedipine, and nicardipine, but not verapamil, were significantly lower versus their respective controls (ACh alone) (**$p < 0.01$, $n = 6$). Brief removal of L-type channel blockers re-sensitized ACh-induced

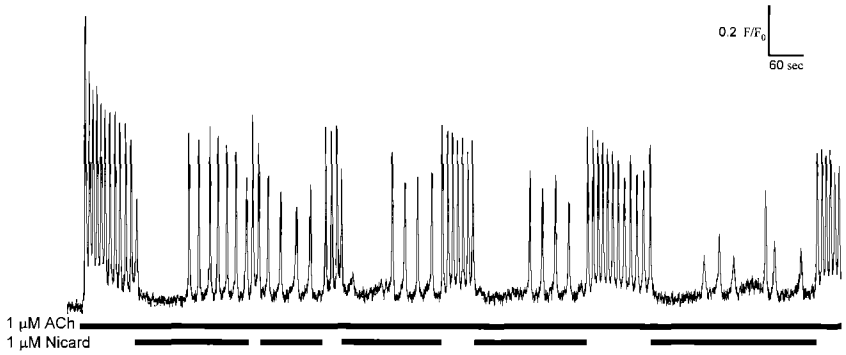

Figure 4. Re-sensitization of ACh-induced $[Ca^{2+}]_i$ oscillations to the inhibitory effect of L-type channel blockers. After ACh-induced $[Ca^{2+}]_i$ oscillations become tolerant to 1 μM nicardipine, brief removal of nicardipine restored sensitivity to L-type channel blockade. Nicardipine-free breaks of 15, 30, 60, and 120 s were tested. The result showed that a nicardipine-free break of minimally 15–30 s was required to re-sensitize the response of ACh-induced $[Ca^{2+}]_i$ oscillations to nicardipine. The $[Ca^{2+}]_i$ trace shown is representative of results in 9 cells from three different animals.

$[Ca^{2+}]_i$ oscillations to inhibition by these agent, as exemplified by nicardipine (1 μM) in Figure 4. Nicardipine-free breaks of 15, 30, 60, and 120 s were tested. The results showed that a minimal nicardipine-free break of >15 s was required to re-sensitize the response of ACh-induced $[Ca^{2+}]_i$ oscillations to 1 μM nicardipine (Figure 4; n = 9 cells from three different animals). After ACh-induced $[Ca^{2+}]_i$ oscillations became tolerant to one L-type channel blocker (1 μM), they were also tolerant to other L-type channel blockers at the same concentration (Figure 5), suggesting the conditions leading to the development of tolerance to the first agent remained in place.

Roles of NCX and NSCC in ACh-induced $[Ca^{2+}]_i$ oscillations and the development of tachyphylaxis to L-type Channel Blockade

Dai et al. [14] demonstrated that, while nifedipine only slightly reduced ACh-mediated tonic contraction and the frequency of $[Ca^{2+}]_i$ oscillations,

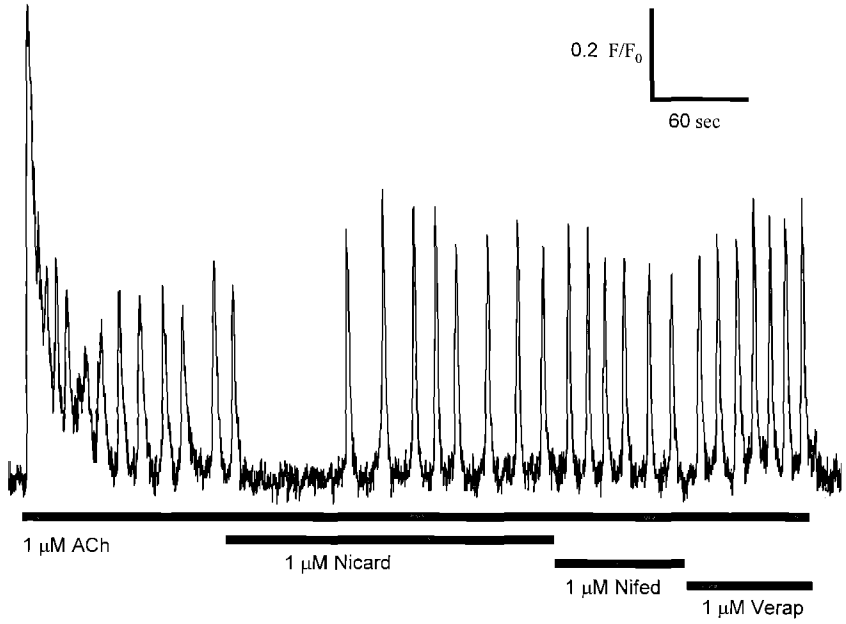

Figure 5. Effect of different L-type channel blockers on ACh-induced $[Ca^{2+}]_i$ oscillations after the development of tachyphylaxis. After ACh-induced $[Ca^{2+}]_i$ oscillations become tolerant to one L-type channel blocker, they were also tolerant to other L-type channel blockers at similar concentrations. (n = 9 cell from three animals).

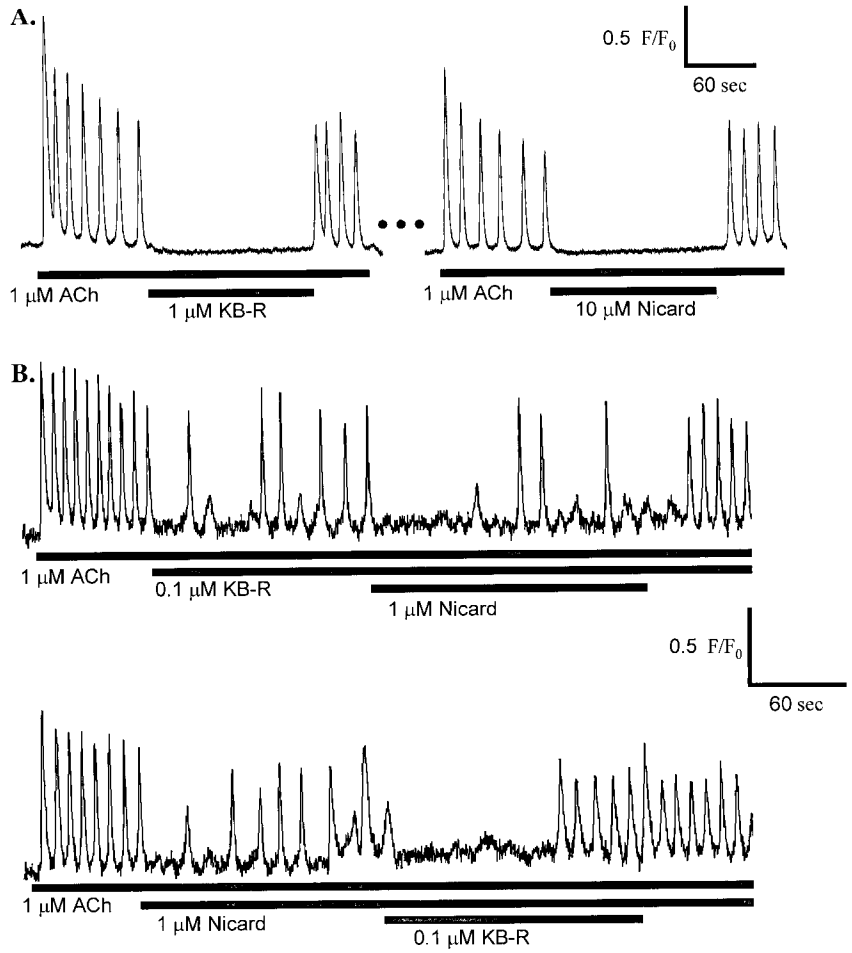

Figure 6. Comparison of the inhibitory effect on ACh-induced $[Ca^{2+}]_i$ oscillations between NCX blocker and L-type channel blocker. A: ACh-induced $[Ca^{2+}]_i$ oscillations were inhibited by 1 μM KB-R7943, an inhibitor of the reverse mode of NCX, as well as 10 μM nicardipine. The two $[Ca^{2+}]_i$ traces shown are two sections from one recording on the same cell separated by 3 min of wash in PSS. These data are representative of results in 8 cells from three different animals. B: Lower concentrations of KB-R7943 (0.1 μM), and nicardipine (1 μM) were used to examine the independent effects of inhibiting L-type VGCC and the reverse mode of NCX during ACh-induced $[Ca^{2+}]_i$ oscillations. Either agents alone at the lower concentrations was be able to temporarily block ACh-induced $[Ca^{2+}]_i$ oscillations. The tolerant part of $[Ca^{2+}]_i$ oscillations was blocked again when the other agent was added, though afterward $[Ca^{2+}]_i$ oscillations still occurred in the presence of both agents (n = 5 cells from two animals). This result demonstrates that both L-type VGCC and the reverse mode of NCX are active and important during ACh-induced $[Ca^{2+}]_i$ oscillations.

the nifedipine-insensitive component was completely blocked by the SK-F96365, an inhibitor of store-operated channels, and almost completely inhibited by KB-R7943, an inhibitor of the reverse mode of NCX. These findings led us to hypothesize that tachyphylaxis of ACh-induced $[Ca^{2+}]_i$ oscillations to L-type channel blockers results from the enhancement of the reverse mode of NCX through the accumulation of intracellular Na^+ via store-operated NSCC. To examine this hypothesis, we first test the relationship between the two pathways of Ca^{2+} entry: L-type VGCC and the reverse mode of NCX. We found that $[Ca^{2+}]_i$ oscillations tolerant to the inhibition of 10 μM nicardipine were blocked by 10 μM KB-R7943 for at least 5 min (n = 5 cells from two animals, data not shown). Actually, KB-R7943 alone at 1 μM was capable of blocking ACh-induced $[Ca^{2+}]_i$ oscillations for at least 2 min (n = 8 cells from three animals, Figure 6A). The concentration of KB-R7943 used by Dai et al. [14] in their study was 20 μM. However, it were

reported that KB-R7943 at 10 μM also suppressed the activity of several other types of channels, especially L-type VGCC [16, 17]. To reduce the non-selective effects of KB-R7943 and nicardipine, we used lower concentrations of the two agents (0.1 μM KB-R7943, and 1 μM nicardipine) to examine the roles of L-type VGCC and the reverse mode of NCX during ACh-induced $[Ca^{2+}]_i$ oscillations (Figure 6B). We found that either agent alone at the lower concentration was able to temporarily block ACh-induced $[Ca^{2+}]_i$ oscillations. The tolerant part of $[Ca^{2+}]_i$ oscillations was blocked again when the other agent was added, though afterward $[Ca^{2+}]_i$ oscillations still recurred in the presence of both agents (Figure 6B, $n = 5$ cells from two animals). These results demonstrate that both L-type VGCC and the reverse mode of NCX are active and important during $[Ca^{2+}]_i$ oscillations.

To further explore the role of NCX in the development of tachyphylaxis to L-type channel blockers, we next examine whether enhancement of the reverse mode of NCX can help regain $[Ca^{2+}]_i$ oscillations. After ACh-induced $[Ca^{2+}]_i$ oscillations were abolished by 10 μM nicardipine, cells were exposed to zero Na^+ buffer to drive currents through NCX in the reverse mode (Figure 7). In the absence of ACh, exposure to zero Na^+ buffer caused a slow increase in baseline $[Ca^{2+}]_i$, without any transient ($n = 5$ cells from two animals, data not shown). During the inhibition of ACh-induced $[Ca^{2+}]_i$ oscillations by 10 μM nicardipine, exposure to zero Na^+ buffer immediately increased $[Ca^{2+}]_i$, and restored $[Ca^{2+}]_i$ oscillations (Figure 7, $n = 7$ cells from two animals). This effect of zero Na^+ buffer was blocked by 10 μM KB-R7943, which indicates that Ca^{2+} influx through the reverse mode of NCX was responsible for the increase in $[Ca^{2+}]_i$, and resumption of $[Ca^{2+}]_i$ oscillations. Since removal of external Na^+ eliminates the competition from Na^+, thus favoring Ca^{2+} entry through NSCC, we examined if NSCC contributes to the resumption of $[Ca^{2+}]_i$ oscillations. Gadolinium is known to block NSCC, and is relatively selective at about 1 μM [18, 19]. In our study, 10 μM Gd^{3+} was used to block Ca^{2+} entry through NSCC. As shown in the lower panel of Figure 7, $[Ca^{2+}]_i$ oscillations recovered by zero Na^+ buffer were not affected by 10 μM Gd^{3+} ($n = 5$ cells from two animals). This result demonstrated that after being inhibited by an L-type channel blocker, ACh-induced $[Ca^{2+}]_i$ oscillations can be recovered through enhancement of the reverse mode of NCX. However, for a condition favoring the reverse mode of NCX to occur, either external $[Na^+]$ has to decrease or the internal $[Na^+]$ has to increase.

It was shown that store-operated NSCC and NCX were the two major Na^+ entry routes in arterial myocytes [20]. We, therefore, explored the possibility that removal of external Ca^{2+} would increase Na^+ entry through NSCC. In the presence of ACh, cells undergoing $[Ca^{2+}]_i$ oscillations were exposed to 10 μM nicardipine in Ca^{2+}-free buffer for 2 min before re-introducing normal (2 mM) Ca^{2+} into the external buffer. In six cells tested by this protocol, only two showed increases in baseline $[Ca^{2+}]_i$ (Figure 8) after re-introduction of normal Ca^{2+} buffer; for the rest of the cells, no significant effect was seen. The increases in $[Ca^{2+}]_i$ in the two responsive cells, however, were not blocked by 1 μM Gd^{3+}, suggesting that the effect was not due to store-operated NSCC. Furthermore, the increase in $[Ca^{2+}]_i$ was inhibited by 1 μM KB-R7943, indicating that a major part of this effect is contributed by NCX (Figure 8). These results suggested that the activity of store-operated NSCC may remain minimal when $[Ca^{2+}]_i$ oscillations were blocked by L-type channel blockers.

To further test our hypothesis, we examine the effect 1 μM Gd^{3+} on ACh-induced $[Ca^{2+}]_i$ oscillations, and the development of tachyphylaxis to the blockade of L-type VGCC and/or NCX. First, cells were exposed to 1 μM Gd^{3+} for 2 min in the presence of 1 μM ACh alone, after ACh-induced $[Ca^{2+}]_i$ oscillations reached a steady state. Then, the effect of 2-min exposure to 1 μM Gd^{3+} were assayed again after ACh-induced $[Ca^{2+}]_i$ oscillations became tolerant to 10 μM nifedipine and "10 μM nifedipine + 1 μM KB-R7943" (Figure 9A). The frequency of $[Ca^{2+}]_i$ oscillations during the 2-min exposure to 1 μM Gd^{3+} were compared and normalized to that in the preceding two minutes. The percentage changes in frequency were evaluated. We found that in the presence of 1 μM ACh alone, 1 μM Gd^{3+} slightly but significantly (***$p < 0.001$) reduced the frequency of ACh-induced $[Ca^{2+}]_i$ oscillations (Figure 9B; $\Delta\% = 19 \pm 2\%$; $n = 5$ cells from two animals), suggesting that Ca^{2+} influx might be partially blocked by 1 μM Gd^{3+}. However, after ACh-induced $[Ca^{2+}]_i$ oscillations became tolerant to

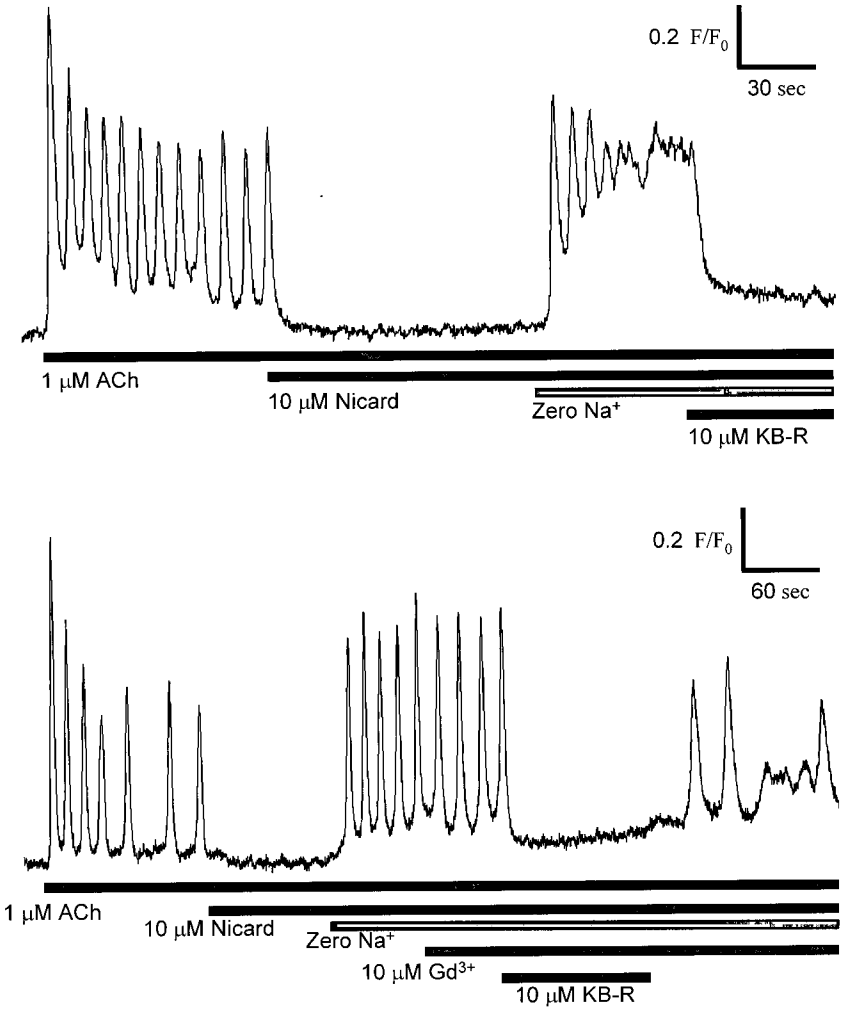

Figure 7. Effect of zero Na^+ buffer and KB-R7943 on the inhibition of ACh-induced $[Ca^{2+}]_i$ oscillations by L-type channel blocker. After ACh-induced $[Ca^{2+}]_i$ oscillations were abolished by 10 μM nicardipine, exposure to zero Na^+ buffer immediately increased $[Ca^{2+}]_i$, and recovered $[Ca^{2+}]_i$ oscillations. The effect of zero Na^+ buffer was not affected by 10 μM Gd^{3+} (lower panel), but was blocked by 10 μM KB-R7943, which indicates that Ca^{2+} influx through the reverse mode of NCX, but not Ca^{2+} entry through NSCC, was responsible for the increase in $[Ca^{2+}]_i$, and resumption of $[Ca^{2+}]_i$ oscillations. This demonstrates that Ca^{2+} entry through the reverse mode of NCX can compensate for the loss of Ca^{2+} due to L-type channel blockers. The $[Ca^{2+}]_i$ traces shown are representative of results in 7 cells from two different animals.

10 μM nifedipine, 1 μM Gd^{3+} significantly increased the frequency of $[Ca^{2+}]_i$ oscillations ($\Delta\% = 81 \pm 6\%$; $^{***}p < 0.001$, $n = 5$ cells from two animals). The positive effect of 1 μM Gd^{3+} on the frequency of $[Ca^{2+}]_i$ oscillations was even more obvious when both L-type VGCC and the reverse mode of NCX were blocked ($\Delta\% = 101 \pm 8\%$; $^{***}p < 0.001$, $n = 5$ cells from two animals). These outcomes may result from the fact that Gd^{3+} can non-selectively block both influx and efflux of Ca^{2+}.

Discussion

The role of L-type VGCC during $[Ca^{2+}]_i$ oscillations has been controversial. Some studies showed complete inhibition of oscillations by L-type channels blockers [13, 21]; some showed only partial inhibition or little effect [14, 22, 23]. In this study, we demonstrated that $[Ca^{2+}]_i$ oscillations induced by 1 μM ACh were at least temporarily abolished by L-type channel blockers (Figure 1). By using the DAD12 Superfusion System, with the tip of its

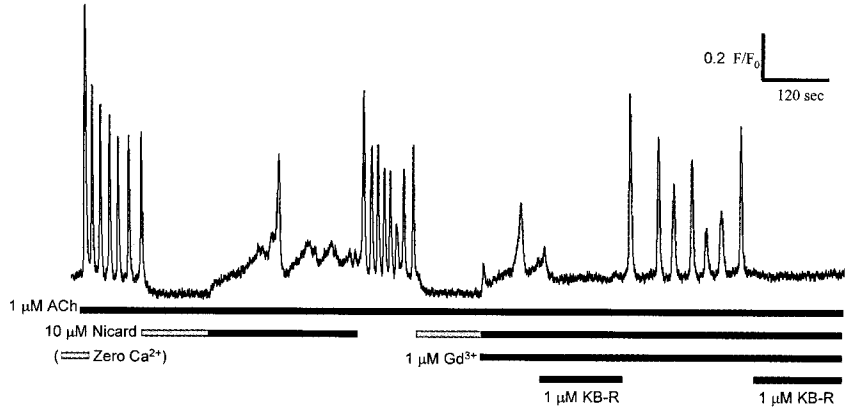

Figure 8. Effect of KB-R7943 on the increase of $[Ca^{2+}]_i$ resulting from temporary deprivation of external Ca^{2+} during the inhibition of ACh-induced $[Ca^{2+}]_i$ oscillations by 10 μM nicardipine. To increase the activity of store-operated NSCC, external Ca^{2+} was temporarily removed during the inhibition of ACh-induced $[Ca^{2+}]_i$ oscillations by 10 μM nicardipine. In six cells tested by this protocol, only two showed increases in baseline $[Ca^{2+}]_i$ after re-exposed to normal Ca^{2+}; for the rest of the cells, no significant effect was seen (data not shown). Here, the result of a cell with increased $[Ca^{2+}]$ after re-exposure to normal PSS is shown. The increase in $[Ca^{2+}]_i$ was not blocked by 10 μM Gd^{3+}, which implied that the major Ca^{2+} influx during this process was not through NSCC. Furthermore, the increase in $[Ca^{2+}]_i$ was completely inhibited by 1 μM KB-R7943, indicating that Ca^{2+} influx through NCX was the major source for the increase in $[Ca^{2+}]_i$ during this process.

micromanifold closely positioned to the target cells we were able to see the inhibitory effect of L-type channel blockers within 1 or 2 s after the application of these agents. The effect of L-type channel blockade on ACh-induced $[Ca^{2+}]_i$ oscillations was rapid and reversible (Figure 1), suggesting that Ca^{2+} influx through L-type VGCC is essential for the maintenance of $[Ca^{2+}]_i$ oscillations. However, further studies using 10 μM ACh (Figure 2A) showed that Ca^{2+} influx through L-type VGCC might be dispensable for producing $[Ca^{2+}]_i$ transients, especially for those induced by higher concentrations of ACh. Even though $[Ca^{2+}]_i$ oscillations induced by 1 μM ACh were abolished by 10 μM nicardipine, cells were still able to quickly respond to 10 μM ACh with large initial $[Ca^{2+}]_i$ transients (Figure 2A), indicating that the abolition of $[Ca^{2+}]_i$ oscillations induced by 1 μM ACh did not occur as a result of the depletion of internal Ca^{2+} store. In TSMCs, ACh-induced $[Ca^{2+}]_i$ oscillations were demonstrated to be mediated by the activation of IP_3 receptors (IP_3R) by IP_3 [24–26]. It has been shown that IP_3R activity is also regulated biphasically by changes in the cytoplasmic Ca^{2+} concentration: Ca^{2+} at submicromolar concentrations potentiates IP_3-induced Ca^{2+} release, while Ca^{2+} at higher concentrations inhibits it [27–30]. Calcium transients provoked by IP_3 (photolysed from the caged compound) were shown to be significantly reduced when immediately preceded by a depolarization (−70 to + 10 mV) pulse that had induced a Ca^{2+} transient [31], suggesting that Ca^{2+} entry via VGCC may cause Ca^{2+} release from IP_3-sensitive store. These findings along with our result suggest that Ca^{2+} influx through L-type VGCC may facilitate Ca^{2+} release from IP_3R when the production of IP_3 is low, and hence is important particularly for $[Ca^{2+}]_i$ transients induced by lower concentrations of ACh.

Even in the absence of external Ca^{2+}, 10 μM ACh was able to evoke $[Ca^{2+}]_i$ transients, though they soon waned (Figure 2A). Calcium transients induced in a Ca^{2+}-free buffer should generally reflect Ca^{2+} release from internal Ca^{2+} stores only. Our data showed that the estimated total $[Ca^{2+}]_i$ transients induced by 10 μM ACh in the presence of 10 μM nicardipine was significantly higher than that in the absence of external Ca^{2+} (Figure 2B). The significant difference in the results can be accounted for by Ca^{2+} entry from the external space, suggesting that even with L-type channels blocked, other pathways of Ca^{2+} entry exist to support $[Ca^{2+}]_i$ transients induced by 10 μM ACh.

In the present study, we also demonstrated tachyphylaxis of ACh-induced $[Ca^{2+}]_i$ oscillations to L-type channel blockers (Figure 3A). Although ACh-induced $[Ca^{2+}]_i$ transients were initially abolished by L-type channel blockers, within minutes, they were able to escape from the

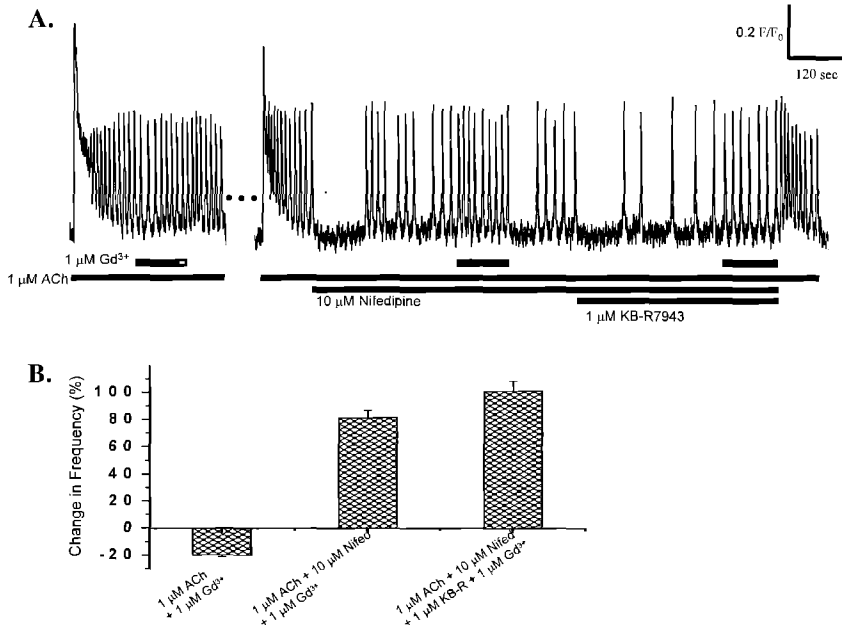

Figure 9. Effect of 1 μM Gd^{3+} on ACh-induced $[Ca^{2+}]_i$ oscillations and tachyphylaxis to blockers of L-type VGCC and/or NCX. Cells were first exposed to 1 μM Gd^{3+} for 2 min in the presence of 1 μM ACh alone after $[Ca^{2+}]_i$ oscillations had reached a steady state. Then, the effect of two-minutes exposure to 1 μM Gd^{3+} were assayed again after ACh-induced $[Ca^{2+}]_i$ oscillations became tolerant to 10 μM nifedipine and to "10 μM nifedipine + 1 μM KB-R7943". The frequency of $[Ca^{2+}]_i$ oscillations during the 2-min exposure to 1 μM Gd^{3+} were compared and normalized to that in the preceding 2 min. The percentage changes in frequency were evaluated. In the presence of 1 μM ACh alone, 1 μM Gd^{3+} slightly reduced the frequency of ACh-induced $[Ca^{2+}]_i$ oscillations (B, n = 5 cells from two animals). However, after ACh-induced $[Ca^{2+}]_i$ oscillations became tolerant to 10 μM nifedipine, 1 μM Gd^{3+} significantly increased the frequency of $[Ca^{2+}]_i$ oscillations ($\Delta\%$ = 81 ± 6%; ***$p < 0.001$, n = 5 cells from two animals). The positive effect of 1 μM Gd^{3+} on the frequency of $[Ca^{2+}]_i$ oscillations was even more obvious when both L-type VGCC and the reverse mode of NCX were blocked ($\Delta\%$ = 101 ± 8%; ***$p < 0.001$, n = 5 cells from two animals).

inhibition by these agents. The recovered $[Ca^{2+}]_i$ transients oscillated at a lower frequency, which further supports our earlier proposal that Ca^{2+} influx through L-type VGCC, though not critical for replenishment of internal stores, may facilitate Ca^{2+} release from IP_3Rs. After ACh-induced $[Ca^{2+}]_i$ oscillations of a cell became tolerant to an L-type channel blocker, brief (15–30 s) removal of the L-type channel blocker re-sensitized the cell to its inhibitory effect on $[Ca^{2+}]_i$ oscillations (Figure 4), whereas switching from one type of L-type channel blocker to another failed to re-sensitize the cells after ACh-induced $[Ca^{2+}]_i$ oscillations already became tolerant to the first one (Figure 5). The re-sensitization most likely represents wash-off of blocker and recovery of calcium levels.

Dai et al. [14] reported that the nifedipine-insensitive component of ACh-induced $[Ca^{2+}]_i$ oscillations was completely inhibited by the inhibitor of store-operated NSCC, SK-F96365, and almost completely inhibited by the inhibitor of the reverse mode of NCX, KB-R7943. Sodium entry via store-operated NSCCs has been shown to have an enormous effect on cell-wide Ca^{2+} signaling, presumably through NCX [20, 32–36]. These findings led us to hypothesize that the reverse mode of NCX is a compensatory pathway for Ca^{2+} entry during L-type channel blockade, which may be enhanced through the accumulation of intracellular Na^+ via NSCC. We demonstrated in this study that $[Ca^{2+}]_i$ oscillations after being abolished by L-type channel blockade resumed immediately when the external solution was switched from normal PSS to zero-Na^+ buffer (Figure 7). This effect of zero-Na^+ buffer was abolished by KB-R7943, suggesting that enhancing the reverse mode of NCX can recover $[Ca^{2+}]_i$ oscillations from the inhibition of L-type channel blockers. Switching to zero-Na^+ buffer should also facilitate Ca^{2+} entry through NSCC. In our study, however, $[Ca^{2+}]_i$ oscillations recovered by

zero-Na^+ buffer were not inhibited by Gd^{3+}, which is known to block NSCC [18, 19].

Our data also demonstrated that KB-R7943 alone was able to abolish $[Ca^{2+}]_i$ oscillations (Figure 6). Interestingly, at ≤ 1 μM tachyphylaxis to KB-R7943 was also observed. Although KB-R7943 is generally accepted as a specific inhibitor of the reverse mode of NCX, it was recently reported to greatly suppress L-type Ca^{2+} currents in cardiomyocytes at concentrations higher than 10 μM [16, 17]. To avoid this nonselective effect, we have used concentrations ≤ 1 μM in most of our studies, though our preliminary data showed that at 10 μM, KB-R7943 was able to completely abolish ACh-induced $[Ca^{2+}]_i$ oscillations for at least 5 min. If the inhibition of ACh-induced $[Ca^{2+}]_i$ oscillations by KB-R7943 can be mainly attributed to the blockade of the reverse mode of NCX, then how can NCX be activated, and driven in the reverse mode during $[Ca^{2+}]_i$ oscillations?

Based on its stoichiometry of 3 Na^+/1 Ca^{2+}, Ca^{2+} entry through NCX is generally regulated according to the following equation:

$$[Ca^{2+}]_i/[Ca^{2+}]_o = ([Na^+]_i/[Na^+]_o)^3 \times e^{(EmF/RT)}$$

where F is the Faraday constant, R is the gas constant, and T is absolute temperature [36–39]. This equation indicates that for NCX to work in reverse mode, increasing the intracellular Na^+ load is the most efficient way, since $[Ca^{2+}]_i$ is proportional to $[Na^+]_i^3$ if other factors remain constant. Store-operated NSCC has been demonstrated to be a major Na^+ entry pathway in arterial myocytes [20]. It is believed that internal Ca^{2+} stores must be depleted in order to activate NSCC [40, 41]. However, it was also reported that during agonist-induced $[Ca^{2+}]_i$ oscillations, calcium content in SR/ER was generally not depleted [8]. Our data showed that KB-R7943 was as effective as L-type channel blockers in blocking ACh-induced $[Ca^{2+}]_i$ oscillations whenever it was added (Figure 6), which means NCX may be constantly active during $[Ca^{2+}]_i$ oscillations. It is unlikely that $[Na^+]_i$ can remain high through the duration of ACh application, since high $[Na^+]_i$ should cause a prolonged Ca^{2+} influx right after the termination of ACh , which does not occur.

On the other hand, even without increase in $[Na^+]_i$,, NCX can still be driven by changes in membrane potential. It has been suggested that the forward mode of NCX may dominate at the resting membrane potential while the reverse mode may prevail when the cell is depolarized [42, 43]. The operation of NCX is electrogenic, based on its stoichiometry of 3 Na^+/1 Ca^{2+}. If the two modes of NCX are in steady state at the resting membrane potential, then depolarization, which normally favors an outward current, should enhance the reverse mode of NCX. Simply put, membrane depolarization is sufficient to result in Ca^{2+} entry through NCX. Since ACh is known to induce depolarization in airway smooth muscle [44], and agonist-induced $[Ca^{2+}]_i$ oscillations are always accompanied by oscillations in membrane potentials [45, 46], it seems reasonable that Ca^{2+} entry through both L-type VGCC and the reverse mode of NCX are involved in the maintenance of $[Ca^{2+}]_i$ oscillations.

Most reports using cells from various tissues showed that Ca^{2+} influx is indispensable for the maintenance of agonist-induced $[Ca^{2+}]_i$ oscillations. However, there are still data showing that, under certain circumstances the oscillations can persist in the absence of extracellular Ca^{2+}. By using La^{3+} to block both the influx and efflux of Ca^{2+}, agonist-induced $[Ca^{2+}]_i$ oscillations were reported to either be terminated or become self-sustained, depending on the cell type [13, 47–49], and in certain cells, also depending on the status of Ca^{2+} load at the point when La^{3+} is applied [50]. Another lanthanide, Gd^{3+}, was also shown to have similar effect at higher concentrations [51]. But, at low ($\sim$1 μM) concentration, it was reported to selectively block store-operated NSCC [18, 19]. In this study, we found that 1 μM Gd^{3+}, when applied in the presence of 1 μM ACh alone slightly reduced the frequency of ACh-induced $[Ca^{2+}]_i$ oscillations (Figure 9). However, in the presence of L-type channel and/or NCX blockers, 1 μsM Gd^{3+} actually enhanced $[Ca^{2+}]_i$ oscillations during tachyphylaxis (Figure 9). Gadolinium has no reported positive effect on Ca^{2+} influx. This effect of Gd^{3+} apparently resulted from the inhibition of Ca^{2+} extrusion. The reason that this effect of Gd^{3+} was more prominent only in the presence of L-type channel and NCX blockers may be twofold: (1) Ca^{2+} influx might already have been largely blocked by L-type channel and NCX blockers so that the additional inhibitory effect contributed by 1 μM Gd^{3+} made no more

difference. (2) The mechanism of Ca^{2+} re-uptake might have been upgraded so that a small deceleration in Ca^{2+} extrusion could lead to a significant improvement in Ca^{2+} recycling.

In summary, our findings suggest that Ca^{2+} entry through L-type VGCC and the reverse mode of NCX are the primary sources of Ca^{2+} for the maintenance of ACh-induced $[Ca^{2+}]_i$ oscillations in TSMCs. The two pathways complement each other, since inhibition of $[Ca^{2+}]_i$ oscillations by blocking one pathway can be reversed by increasing the activity of the other. Enhanced recycling of internal Ca^{2+} due in part to reduced efflux may result in the development of tachyphylaxis to both the inhibitors of L-type VGCC and the reverse mode of NCX.

References

1. Lee C.H., Kuo K.H., Dai J. and van Breemen C., Asynchronous calcium waves in smooth muscle cells. Can. J. Physiol. Pharmacol. 83(8–9) 733–741, 2005.
2. Malcuit C., Kurokawa M. and Fissore R.A., Calcium oscillations and mammalian egg activation. J. Cell Physiol. 206(3) 565–573, 2006.
3. Ikeda M, Calcium dynamics and circadian rhythms in suprachiasmatic nucleus neurons. Neuroscientist 10(4) 315–324, 2004.
4. Halet G., Marangos P., Fitzharris G. and Carroll J., Ca^{2+} oscillations at fertilization in mammals. Biochem. Soc. Trans. 31(Pt 5) 907–911, 2003.
5. Guse A.H., Ca^{2+} signaling in T-lymphocytes. Crit. Rev. Immunol. 18(5) 419–448, 1998.
6. Bergsten P., Lin J. and Westerlund J., Pulsatile insulin release: role of cytoplasmic Ca^{2+} oscillations. Diabetes Metab. 24(1) 41–45, 1998.
7. Kuo K.H., Dai J., Seow C.Y., Lee C.H. and van Breemen C., Relationship between asynchronous Ca^{2+} waves and force development in intact smooth muscle bundles of the porcine trachea. Am. J. Physiol. Lung Cell. Mol. Physiol. 285(6) L1345–L1353, 2003.
8. Shuttleworth T.J., What drives calcium entry during $[Ca^{2+}]$i oscillations? – challenging the capacitative model. Cell Calcium 25(3) 237–246, 1999.
9. Lee C.H., Poburko D., Kuo K.H., Seow C. and van Breemen C. Relationship between the sarcoplasmic reticulum and the plasma membrane. Novartis Found. Symp. 246: 26–41; discussion 41–7, 48–51, 2002.
10. Janssen L.J., Wattie J., Lu-Chao H. and Tazzeo T., Muscarinic excitation–contraction coupling mechanisms in tracheal and bronchial smooth muscles. J. Appl. Physiol. 91(3) 1142–1151, 2001.
11. Farley J.M. and Miles P.R., The sources of calcium for acetylcholine-induced contractions of dog tracheal smooth muscle. J. Pharmacol. Exp. Ther. 207(2) 340–346, 1978.
12. Shieh C.C., Petrini M.F., Dwyer T.M. and Farley J.M., Calcium mobilization and muscle contraction induced by acetylcholine in swine Trachealis. J. Biomed. Sci. 2(3) 272–282, 1995.
13. Prakash Y.S., Kannan M.S. and Sieck G.C., Regulation of intracellular calcium oscillations in porcine tracheal smooth muscle cells. Am. J. Physiol. 272(3 Pt 1) C966–C975, 1997.
14. Dai J.M., Kuo K.H., Leo J.M., van Breemen C. and Lee C.H., Mechanism of ACh-induced asynchronous calcium waves and tonic contraction in porcine tracheal muscle bundle. Am. J. Physiol. Lung Cell. Mol. Physiol. 290(3) L459–L469, 2006.
15. Julou G. and Freslon J.L., Effects of calcium entry blockers on Ca^{2+}-induced contraction of depolarized and noradrenaline-exposed rat resistance vessels. Eur. J. Pharmacol. 129(3) 261–270, 1986.
16. Birinyi P., Acsai K., Banyasz T., Toth A., Horvath B., Virag L., Szentandrassy N., Magyar J., Varro A., Fulop F. and Nanasi P.P., Effects of SEA0400 and KB-R7943 on Na^+/Ca^{2+} exchange current and L-type Ca^{2+} current in canine ventricular cardiomyocytes. Naunyn Schmiedebergs Arch. Pharmacol. 372(1) 63–70, 2005.
17. Tanaka H., Nishimaru K., Aikawa T., Hirayama W., Tanaka Y. and Shigenobu K., Effect of SEA0400, a novel inhibitor of sodium–calcium exchanger, on myocardial ionic currents. Br. J. Pharmacol. 135(5) 1096–1100, 2002.
18. Putney J.W. Jr., Pharmacology of capacitative calcium entry. Mol. Interv. 1(2) 84–94, 2001.
19. Bird G.S. and Putney J.W. Jr., Capacitative calcium entry supports calcium oscillations in human embryonic kidney cells. J. Physiol. 562(Pt 3) 697–706, 2005.
20. Arnon A., Hamlyn J.M. and Blaustein M.P., Na^+ entry via store-operated channels modulates Ca^{2+} signaling in arterial myocytes. Am. J. Physiol. Cell Physiol. 278(1) C163–C173, 2000.
21. Kohda M., Komori S., Unno T. and Ohashi H., Carbachol-induced $[Ca^{2+}]$i oscillations in single smooth muscle cells of guinea-pig ileum. J. Physiol. 492(Pt 2) 315–328, 1996.
22. Lee C.H., Poburko D., Sahota P., Sandhu J., Ruehlmann D.O. and van Breemen C., The mechanism of phenylephrine-mediated $[Ca^{2+}]$i oscillations underlying tonic contraction in the rabbit inferior vena cava. J Physiol. 534(Pt 3) 641–650, 2001.
23. Kajioka S., Nakayama S., Asano H. and Brading A.F., Involvement of ryanodine receptors in muscarinic receptor-mediated membrane current oscillation in urinary bladder smooth muscle. Am. J. Physiol. Cell Physiol. 288(1) C100–C108, 2005.
24. Liu X. and Farley J.M., Acetylcholine-induced Ca^{++}-dependent chloride current oscillations are mediated by inositol 1,4,5-trisphosphate in tracheal myocytes. J. Pharmacol. Exp. Ther. 277(2) 796–804, 1996.
25. Chopra L.C., Twort C.H., Cameron I.R. and Ward J.P., Inositol 1,4,5-trisphosphate- and guanosine 5′-O-(3-thiotriphosphate)-induced Ca^{2+} release in cultured airway smooth muscle. Br. J. Pharmacol. 104(4) 901–906, 1991.
26. Kannan M.S., Prakash Y.S., Brenner T., Mickelson J.R. and Sieck G.C., Role of ryanodine receptor channels in Ca^{2+} oscillations of porcine tracheal smooth muscle. Am. J. Physiol. 272(4 Pt 1) L659–L664, 1997.
27. Iino M, Biphasic Ca^{2+} dependence of inositol 1,4,5-trisphosphate-induced Ca^{2+} release in smooth muscle cells of the guinea pig taenia caeci. J. Gen. Physiol. 95: 1103–1122, 1990.
28. Bezprozvanny I., Watras J. and Ehrlich B.E., Bell-shaped calcium-response curve of Ins(1,4,5)P3- and calcium-gated channels from endoplasmic reticulum of cerebellum. Nature 351: 751–754, 1991.

29. Finch E.A., Turner T.J. and Goldin S.M., Calcium as a coagonist of inositol 1,4,5-trisphosphate-induced calcium release. Science 252: 443–446, 1991.
30. Bootman M.D., Missiaen L., Parys J.B., De Smedt H. and Casteels R., Control of inositol 1,4,5-trisphosphate-induced Ca^{2+} release by cytosolic Ca^{2+}. Biochem. J. 306: 445–451, 1995.
31. McCarron J.G., MacMillan D., Bradley K.N., Chalmers S. and Muir T.C., Origin and mechanisms of Ca^{2+} waves in smooth muscle as revealed by localized photolysis of caged inositol 1,4,5-trisphosphate. J. Biol. Chem. 279(9) 8417–8427, 2004.
32. Arnon A., Hamlyn J.M. and Blaustein M.P., Ouabain augments Ca^{2+} transients in arterial smooth muscle without raising cytosolic Na(+). Am. J. Physiol. Heart Circ. Physiol. 279(2) H679–H691, 2000.
33. Paltauf-Doburzynska J., Frieden M., Spitaler M. and Graier W.F., Histamine-induced Ca^{2+} oscillations in a human endothelial cell line depend on transmembrane ion flux, ryanodine receptors and endoplasmic reticulum Ca^{2+}-ATPase. J. Physiol. 524(Pt 3) 701–713, 2000.
34. Lee C.H., Poburko D., Kuo K.H., Seow C.Y. and van Breemen C., Ca^{2+} oscillations, gradients, and homeostasis in vascular smooth muscle. Am. J. Physiol. Heart Circ. Physiol. 282(5) H1571–H1583, 2002.
35. Rosker C., Graziani A., Lukas M., Eder P., Zhu M.X., Romanin C. and Groschner K., Ca^{2+} signaling by TRPC3 involves Na^{+} entry and local coupling to the Na^{2}/Ca^{2+} exchanger. J. Biol. Chem. 279(14) 13696–13704, 2004.
36. Zhang S., Yuan J.X., Barrett K.E. and Dong H., Role of Na^{2}/Ca^{2+} exchange in regulating cytosolic Ca^{2+} in cultured human pulmonary artery smooth muscle cells. Am. J. Physiol. Cell Physiol. 288(2) C245–C252, 2005.
37. Hinata M., Yamamura H., Li L., Watanabe Y., Watano T., Imaizumi Y. and Kimura J., Stoichiometry of Na^{2}/Ca^{2+} exchange is 3:1 in guinea-pig ventricular myocytes. J. Physiol. 545(Pt 2) 453–461, 2002.
38. Blaustein M.P., Physiological effects of endogenous ouabain: control of intracellular Ca^{2+} stores and cell responsiveness. Am. J. Physiol. Cell Physiol. 264: C1367–C1387, 1993.
39. Blaustein M.P. and Lederer W.J., Sodium/calcium exchange: its physiological implications. Physiol. Rev. 79: 763–854, 1999.
40. Putney J.W. Jr., Capacitative calcium entry revisited. Cell Calcium 11(10) 611–624, 1990.
41. Parekh A.B. and Putney J.W. Jr., Store-operated calcium channels. Physiol. Rev. 85(2) 757–810, 2005.
42. Piacentino V. 3rd, Weber C.R., Gaughan J.P., Margulies K.B., Bers D.M. and Houser S.R., Modulation of contractility in failing human myocytes by reverse-mode Na^{2}/Ca^{2+} exchange. Ann. NY Acad. Sci. 976: 466–471, 2002.
43. Philipson K.D., Nicoll D.A., Ottolia M., Quednau B.D., Reuter H., John S. and Qiu Z., The Na^{2}/Ca^{2+} exchange molecule: an overview. Ann. NY Acad. Sci. 976: 1–10, 2002.
44. Farley J.M. and Miles P.R., Role of depolarization in acetylcholine-induced contractions of dog trachealis muscle. J. Pharmacol. Exp. Ther. 201(1) 199–205, 1977.
45. Kohda M., Komori S., Unno T. and Ohashi H., Carbachol-induced oscillations in membrane potential and $[Ca^{2+}]i$ in guinea-pig ileal smooth muscle cells. J. Physiol. 511(Pt 2) 559–571, 1998.
46. Choi J. and Farley J.M., Effects of 8-bromo-cyclic GMP on membrane potential of single swine tracheal smooth muscle cells. J. Pharmacol. Exp. Ther. 285(2) 588–594, 1998.
47. Morgan A.J. and Jacob R., Differential modulation of the phases of a Ca^{2+} spike by the store Ca^{2+}-ATPase in human umbilical vein endothelial cells. J. Physiol. 513(Pt 1) 83–101, 1998.
48. Wayman C.P., McFadzean I., Gibson A. and Tucker J.F., Cellular mechanisms underlying carbachol-induced oscillations of calcium-dependent membrane current in smooth muscle cells from mouse anococcygeus. Br. J. Pharmacol. 121(7) 1301–1308, 1997.
49. Kohda M., Komori S., Unno T. and Ohashi H., Carbachol-induced $[Ca^{2+}]i$ oscillations in single smooth muscle cells of guinea-pig ileum. J. Physiol. 492(Pt 2) 315–328, 1996.
50. Sneyd J., Tsaneva-Atanasova K., Yule D.I., Thompson J.L. and Shuttleworth T.J., Control of calcium oscillations by membrane fluxes. Proc. Natl. Acad. Sci. USA 101(5) 1392–1396, 2004.
51. Van Breemen C., Farinas B.R., Gerba P. and McNaughton E.D., Excitation–contraction coupling in rabbit aorta studied by the lanthanum method for measuring cellular calcium influx. Circ. Res. 30(1) 44–54, 1972.